Catalysis Letters Vol. 78, Nos. 1–4, March 2002 (© 2002)

Comparative study on partial oxidation of methane over Ni/ZrO_2, Ni/CeO_2 and $Ni/Ce–ZrO_2$ catalysts

Wen-Sheng Dong *, Ki-Won Jun, Hyun-Seog Roh, Zhong-Wen Liu, and Sang-Eon Park **

Catalysis Center for Molecular Engineering, Korea Research Institute of Chemical Technology, PO Box 107, Yusong, Taejon 305-600, Korea

Received 21 June 2001; accepted 10 October 2001

The partial oxidation of methane has been studied by sequential pulse experiments with $CH_4 \rightarrow O_2 \rightarrow CH_4$ and simultaneous pulse reaction of CH_4/O_2 (2/1) over Ni/CeO_2, Ni/ZrO_2 and $Ni/Ce–ZrO_2$ catalysts. Over Ni/CeO_2, CH_4 dissociates on Ni and the resultant carbon species quickly migrate to the interface of $Ni–CeO_2$, and then react with lattice oxygen of CeO_2 to form CO. A synergistic effect between Ni and CeO_2 support contributes to CH_4 conversion. Over Ni/ZrO_2, CH_4 and O_2 are activated on the surface of metallic Ni, and then adsorbed carbon reacts with adsorbed oxygen to produce CO, which is composed of the main path for the partial oxidation of methane. The addition of ceria to zirconia enhances CH_4 dissociation and improves the carbon storage capacity. Moreover, it increases the storage capacity and mobility of oxygen in the catalyst, thus promoting carbon elimination.

KEY WORDS: pulse reaction; partial oxidation of methane; Ni; CeO_2; ZrO_2; $Ce–ZrO_2$

1. Introduction

The catalytic partial oxidation of methane (POM) to CO and H_2 is of great practical importance in utilization of natural gas. In the past decades, extensive investigations have been made in POM since the reaction is mildly exothermic, highly efficient and can produce synthesis gas with a H_2/CO mole ratio of 2, which is well suitable for the methanol synthesis and the Fischer–Tropsch reaction [1]. It provides a great promise to replace the conventional steam reforming of methane, which is an energy intensive process, for the production of synthesis gas.

It has been reported that high methane conversion, H_2 and CO selectivities can be obtained over a number of metal catalysts such as Rh, Pt, Ru, Ir, Co and Ni [2–7]. The catalysts based on noble metals are known to be more active and less sensitive to coke formation than Ni-based catalysts. However, because of the very high cost of noble-metal-based catalysts, supported Ni catalysts are more promising for industrial utilization.

To develop a high performance catalyst, it is essential to elucidate the reaction mechanism. So far, two mechanisms have been proposed for POM to synthesis gas: (i) The combustion-reforming mechanism, which involves an initially strongly exothermic methane combustion to CO_2 and H_2O, followed by the strongly endothermic reforming reaction of the rest of CH_4 with CO_2 and H_2O to produce synthesis gas [8–10]. (ii) The direct partial oxidation mechanism, in which CO is produced directly without the preformation of CO_2 [3,11–15]. This mechanism involves two steps, namely the pyrolysis $CH_4 \rightarrow C + 4H$, followed by the oxidation of C to CO. Some recent investigations brought support to this mechanism. Hickman and Schmidt [3] investigated Rh- and Pt-impregnated foam monoliths as catalysts for POM. They proposed that the mechanism involved direct formation of H_2 initiated by CH_4 pyrolysis on the surface to give surface C and H species. The H atoms dimerize and desorb as H_2, while the surface C atoms react with adsorbed O atoms and desorb as CO. Au *et al.* [11] compared the reaction behavior of CH_4 and CH_4/O_2 over SiO_2-supported Ni and Cu catalysts using pulse techniques, and suggested that the conversion of CH_4/O_2 to synthesis gas followed the pyrolysis mechanism. According to Hu and Ruckenstein [12], transient response analysis indicated that over Ni/SiO_2 catalyst CH_4 and O_2 react in the adsorbed states *via* the pyrolysis mechanism. They concluded that the reaction between the surface carbon species and the surface oxygen species constitutes the rate-controlling step. Based on the results of pulse reaction of CH_4, CH_4/O_2 and CH_4/CO_2 over Ni/Al_2O_3 catalyst, Lu *et al.* [13] suggested that the primary surface reaction of POM proceeds *via* a CH_4 pyrolysis followed by the reduction of NiO_x by the surface C atoms. Very recently, Jin *et al.* [15] claimed that both CH_4 and O_2 are activated on Ni^0 sites, generating surface $Ni\cdots C$ and $Ni^{\delta+}\cdots O^{\delta-}$ species. The reaction between these two kinds of intermediates generates the primary product of CO.

In our previous studies [16,21], $Ni/Ce–ZrO_2$ exhibited high catalytic performances in POM, SRM and OSRM (combination of POM and SRM). A mechanistic scheme was proposed to explain the excellent performance of $Ni/Ce–ZrO_2$ catalyst.

In this work, we conducted pulse reaction of CH_4, O_2 and CH_4/O_2 to investigate further the reaction performance of Ni/ZrO_2, Ni/CeO_2 and $Ni/Ce–ZrO_2$ catalysts. The results

---

* Present address: Institute of Coal Chemistry, Chinese Academy of Sciences, Taiyuan 030001, PR China.

** To whom correspondence should be addressed. E-mail: separk@krict.re.kr

1011-372X/02/0300-0215/0 © 2002 Plenum Publishing Corporation

allowed us to identify the reaction intermediates and to examine the reaction mechanism.

2. Experimental

2.1. Preparation of the catalysts

Support materials employed in this study were monoclinic ZrO_2 (99%, Strem Chemicals), CeO_2 (99%, Aldrich Chemicals), and Ce-doped ZrO_2. The BET surface areas for ZrO_2 and CeO_2 are 18.4 and 2.0 m^2/g, respectively. Ce-doped zirconia support was prepared by a sol–gel method with ZrO_2 to CeO_2 weight ratio of 4 [21]. The modified support was calcined at 800 °C for 6 h. The BET analysis showed that the surface area of the support is 55.0 m^2/g. The support has a tetragonal phase structure as indicated by XRD patterns. Supported Ni (15 wt%) catalysts were prepared by the molten-salt method as described elsewhere [17].

2.2. Pulse reaction

Pulse experiments using CH_4, O_2 and CH_4/O_2 mixed gas were performed in a quartz flow microreactor with an inner diameter of 4 mm. Prior to the reaction, each catalyst (15 mg) was loaded in the reactor and reduced *in situ* in 5% H_2/N_2 at 700 °C for 3 h. After that, the sample was heated to 800 °C in He (30 ml/min), and held at 800 °C for 90 min to remove any residual gases in the system, then exposed to pulses of CH_4, O_2 or CH_4/O_2 (1 ml pulse, 10–15 min interval). During each pulse, the exit gas was analyzed on-line by a Shimadzu GC-8A gas chromatograph equipped with TCD (carbosphere column, 80 °C; helium as carrier gas). The conversion and selectivity were calculated on the basis of carbon contents in the products and 100% carbon and oxygen balances.

In the present study, CO, CO_2, CO* and CO_2^* selectivities were defined according to the following equations:

$$\text{CO selectivity (\%)} = \frac{\text{moles of CO formed}}{\text{moles of CH}_4\text{ conversion}} \times 100\%,$$

$$\text{CO}_2\text{ selectivity (\%)} = \frac{\text{moles of CO}_2\text{ formed}}{\text{moles of CH}_4\text{ conversion}} \times 100\%,$$

$$\text{CO}^*\text{ selectivity (\%)} = \frac{0.5 \times \text{moles of CO formed}}{\text{moles of O}_2\text{ conversion}} \times 100\%,$$

$$\text{CO}_2^*\text{ selectivity (\%)} = \frac{\text{moles of CO}_2\text{ formed}}{\text{moles of O}_2\text{ conversion}} \times 100\%.$$

3. Results

3.1. Sequential pulse reaction of CH_4 and O_2

In this experiment, five pulses of each gas were injected in a sequence of $CH_4 \rightarrow O_2 \rightarrow CH_4$. The blank runs in an empty tube and CH_4 pulses over ZrO_2, CeO_2 and Ce–ZrO_2 supports showed no CH_4 conversion at 800 °C.

Sequential pulse experiments ($CH_4 \rightarrow O_2 \rightarrow CH_4$) were performed over Ni/ZrO_2, Ni/CeO_2 and Ni/Ce–ZrO_2 catalysts at 800 °C to investigate the CH_4 dehydrogenation activity and carbon elimination by O_2. Figure 1 shows CH_4 (O_2) conversion, CO (CO*) and CO_2 (CO_2^*) selectivities during three sets of pulses. For the methane ordinal pulses, the conversion of methane was the highest in the first pulse, and then decreased with increasing pulse number in different rates over different catalysts. Since the activities of all the catalysts for methane decomposition could be restored to their initial values after removing the carbon species deposited on the catalysts and replenishing the lattice oxygen in the following oxygen pulses, it can be concluded that the decrease of methane conversion over these catalysts can be ascribed to both the deposition of carbon species on the active sites for methane decomposition and the consumption of the reactive oxygen species present on the catalyst. Over Ni/CeO_2 catalyst, the first CH_4 pulse generated a large amount of CO and H_2, but no CO_2 was detected. Since there is no gas-phase oxygen species present in the system, it suggests that the oxygen is from the support. The initial CH_4 conversion was 61.1%, and then declined rapidly to 4% for the third pulse, while the CO selectivity decreased from 55.5 to 0%, indicating that mobile oxygen species in the CeO_2 support were exhausted. In this case, it is plausible to suggest that the decrease of methane conversion over Ni/CeO_2 catalyst mainly resulted from the decrease of the mobile oxygen in the support with methane pulses.

Considering Ni/ZrO_2 and Ni/Ce–ZrO_2 catalysts, in the first CH_4 pulse, a large amount of H_2 and a very small amount of CO were detected. The CO selectivities for the first pulse were 1.6 and 3.7%, respectively, implying that the reducible oxygen species in both Ni/ZrO_2 and Ni/Ce–ZrO_2 catalysts are much less than that in Ni/CeO_2 after the reduction at 700 °C for 3 h. CH_4 conversion was 65.2% over Ni/ZrO_2 and 74.5% over Ni/Ce–ZrO_2 for the first pulse. The results indicate that CH_4 is effectively dissociated to form carbon species, which is confirmed by the effluents, CO and CO_2 when O_2 was pulsed after the 5th CH_4 pulses. With increasing CH_4 pulse, CH_4 conversion decreased gradually over Ni/ZrO_2 catalysts mainly due to the carbon deposited on the catalyst surface since the reactive oxygen species over the catalyst were very scarce. However, the decrease of CH_4 conversion over Ni/Ce–ZrO_2 was the lowest, indicating that Ni/Ce–ZrO_2 catalyst has the best ability to resist deactivation caused by coke formation which is confirmed by the following results (table 1). In the case of Ni/CeO_2, increasing CH_4 pulse number resulted in a sharp decrease of CH_4 conversion along with the decrease of CO selectivity. Once the reducible oxygen species in the catalyst are exhausted, the CH_4 dissociation activity becomes very low. This phenomenon is obviously different from that over Ni/ZrO_2 and Ni/Ce–ZrO_2. Although the reducible oxygen species in Ni/ZrO_2 and Ni/Ce–ZrO_2 at the present conditions were very scarce, these catalysts still showed higher CH_4 dissociation activity. It strongly suggests that CH_4 dissociation occurs on the metallic Ni active sites for Ni/ZrO_2

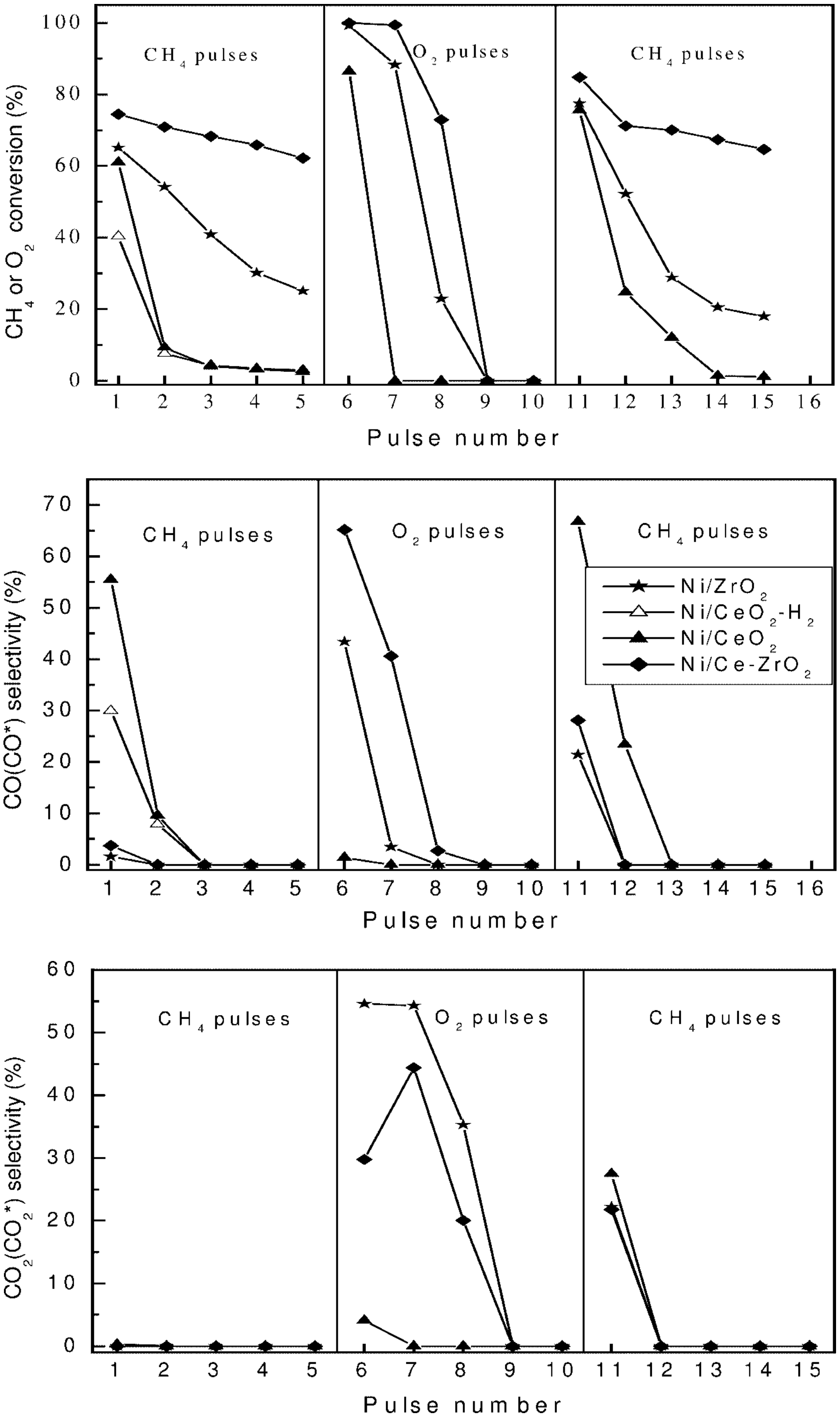

Figure 1. Sequential pulse reaction ($CH_4 \rightarrow O_2 \rightarrow CH_4$) over Ni/CeO_2, Ni/CeO_2–H_2, Ni/ZrO_2 and Ni/Ce–ZrO_2 catalysts at 800 °C (Ni/CeO_2–H_2: the sample was treated with H_2 pulse before CH_4 pulses).

Table 1
The results of sequential pulse reaction of CH_4 and O_2 over supported Ni catalysts

Catalyst	C deposition (mmol)	Removed C (mmol)	C residue (mmol)	Adsorbed O (mmol)
Ni/ZrO_2	0.0958	0.0904	0.0054	0.0483
Ni/CeO_2	0.0202	0.0027	0.0175	0.0729
Ni/Ce–ZrO_2	0.1400	0.1390	0.0010	0.0627

and Ni/Ce–ZrO_2 catalysts and the carbon deposition over the catalysts is responsible for the decrease of methane conversion. However, in the case of Ni/CeO_2, it seems that a synergistic effect between Ni and mobile oxygen species in the CeO_2 support exists for CH_4 conversion. In order to verify this point of view, after reduced Ni/CeO_2 catalyst was purged with He at 800 °C for 90 min, pure H_2 pulses were injected to remove parts of mobile oxygen species in

Ni/CeO_2, and then CH_4 pulses were introduced. The initial CH_4 conversion and CO selectivity were 40.4 and 29.9%, respectively. These values are obviously lower than those over the Ni/CeO_2 which was untreated with pure H_2 pulses. It indicates that the mobile oxygen species in the CeO_2 support play a very important role in CH_4 conversion and CO production over Ni/CeO_2. It also shows that Ni active sites over Ni/CeO_2 have a very weak ability to dissociate CH_4 once the mobile oxygen is exhausted, which is consistent with H_2 uptake of 0.0 μmol/g-cat in our previous H_2 pulse chemisorption experiment [18].

On the basis of 100% carbon and oxygen balances, after each set of reactions in three sets of sequential pulse reaction ($CH_4 \rightarrow O_2 \rightarrow CH_4$), we can calculate the amount of C deposited on the catalysts, the amount of C removed from the catalysts and the amount of O adsorbed on the catalysts. The results are shown in table 1.

After five CH_4 pulses, the amount of carbon deposited over the catalysts decreased in the order $Ni/Ce–ZrO_2 > Ni/ZrO_2 > Ni/CeO_2$ as shown in table 1, indicating that $Ni/Ce–ZrO_2$ has the strongest ability to dissociate CH_4. Meanwhile, during CH_4 pulses, $Ni/Ce–ZrO_2$ showed the lowest deactivation rate. Thus we can reasonably speculate that some carbon species may migrate to the interface between metallic Ni and $Ce–ZrO_2$ support, resulting in slow deactivation. A similar result has been reported by Stagg-Williams *et al.* [19] in CO_2 reforming with methane over the $Pt/Ce–ZrO_2$ system.

To investigate the reaction between surface carbon and O_2, oxygen was pulsed after 5 pulses of CH_4. A large amount of CO and CO_2 was produced in the first O_2 pulse over Ni/ZrO_2 and $Ni/Ce–ZrO_2$ catalysts, indicating the carbon species can react quickly with surface O species to form CO and CO_2. Over $Ni/Ce–ZrO_2$ catalyst, CO^* selectivity was higher, while CO_2^* was lower than those over Ni/ZrO_2. This can be explained as follows. It is believed that the molar ratio of surface carbon to oxygen is a crucial factor to determine the selectivities of CO and CO_2 [14]. The higher the molar ratio of surface carbon to oxygen, the more favorable to the production of CO. In the present cases, the pulsed oxygen was consumed completely over the two catalysts for the first oxygen pulse. At the same time, it is clear that the amount of carbon deposited on $Ni/Ce–ZrO_2$ was higher than that on Ni/ZrO_2 as shown in table 1. So, the molar ratio of surface carbon to oxygen over Ni/ZrO_2 was lower than that over $Ni/Ce–ZrO_2$. This caused the differences of CO and CO_2 selectivities over the two catalysts. With increasing O_2 pulse number, the surface carbon species decrease, while the corresponding oxygen species increase. Thus, the ratio of CO^*/CO_2^* and total quantity of CO and CO_2 decrease. Based on the above results, it is clear that CO is from the surface C species. Thus, one can deduce that the surface C species may be the intermediate for the POM reaction over both Ni/ZrO_2 and $Ni/Ce–ZrO_2$ catalysts.

In the case of Ni/CeO_2, it is very interesting to note that much less CO and CO_2 were generated in the first O_2 pulse, although a large amount of O_2 was consumed, implying that C species deposited on the surface of Ni/CeO_2 are very difficult to remove. So, it is reasonable to suggest that most parts of O_2 are consumed to replenish the lattice oxygen in the CeO_2 support and to oxidize metallic nickel species.

After five O_2 pulses, the amount of carbon residue on the catalysts decreased in the order $Ni/CeO_2 > Ni/ZrO_2 > Ni/Ce–ZrO_2$ as indicated in table 1. It clearly indicates that $Ni/Ce–ZrO_2$ has the best ability to eliminate carbon species. During O_2 pulses, some activated oxygen species adsorbed on the surface of the catalysts. The Ni/CeO_2 catalyst showed the highest O capacity, followed by $Ni/Ce–ZrO_2$ and Ni/ZrO_2.

In order to investigate the oxygen species involved in POM, CH_4 was introduced again after O_2 pulses. It was found that a considerable amount of CO and CO_2 was generated in the first CH_4 pulse. For the first CH_4 pulse in the third set of pulses, CH_4 conversions over the partially oxidized catalysts were higher than those over the freshly reduced catalysts in the first CH_4 pulse. This indicates that the oxygen adsorbed on the catalysts can enhance the conversion of CH_4. The CO selectivity and total yields of CO and CO_2 over the catalysts decreased in the following order: $Ni/CeO_2 > Ni/CeZrO_2 > Ni/ZrO_2$, implying that adsorbed oxygen species over Ni/CeO_2 and $Ni/Ce–ZrO_2$ are more favorable to produce CO and CO_2 than those over Ni/ZrO_2.

3.2. Simultaneous pulse reaction of CH_4/O_2

The CH_4/O_2 (2/1) pulse reactions were performed over ZrO_2, CeO_2 and $Ce–ZrO_2$ supports. During the pulse reaction, the conversions and selectivities over the supports remained almost constant. The results obtained in the second pulse are listed in table 2. The CH_4 was converted prac-

Table 2
Pulse reaction of CH_4/O_2 (2/1) over various supports[a]

Support	Temp. (°C)	CH_4 conv. (%)	O_2 conv. (%)	CO sel. (%)	CO_2 sel. (%)	Cs sel. (%)	$CO_2/(CO + CO_2)$ (%)
ZrO_2	600	6.8	15.1	42.7	25.5	31.8	37.4
	800	31.4	96.3	26.8	52.4	20.8	66.2
CeO_2	600	2.6	7.3	0.0	60.6	39.4	100
	800	27.6	100	2.1	83.1	14.8	97.6
$Ce–ZrO_2$	600	25.8	100	3.0	84.9	12.0	96.6
	800	27.4	100	6.9	80.5	12.6	92.1

[a] Data obtained from the second pulse.

tically into CO_2 over the supports besides the deposition of some carbon-containing species at the same reaction temperature (800 °C). The fact that $Ce–ZrO_2$ showed much higher CH_4 and O_2 conversion than ZrO_2 and CeO_2 at 600 °C confirms further that the formation of active oxygen species over $Ce–ZrO_2$ is much easier to be produced than that over ZrO_2 and CeO_2.

The CH_4/O_2 (2/1) pulse reactions were also performed over Ni/ZrO_2, Ni/CeO_2 and $Ni/Ce–ZrO_2$ catalysts. During the pulse reaction, O_2 was completely converted over all the catalysts. The carbon balance indicates that no obvious carbon deposition took place, implying that the conversion of CH_4 on the pure supports could be neglected. Figure 2 shows the reaction results. The CH_4 conversions over these catalysts at 800 °C were more than 85%, which is much higher than those over pure supports. The activity decreased in the following order: $Ni/CeZrO_2 > Ni/ZrO_2 > Ni/CeO_2$. Meanwhile, all the catalysts showed more than 93% CO selectivities, which is much higher than those over the supports, confirming further that the direct contribution of the supports to the conversion of methane is slight during the CH_4/O_2 pulse reaction.

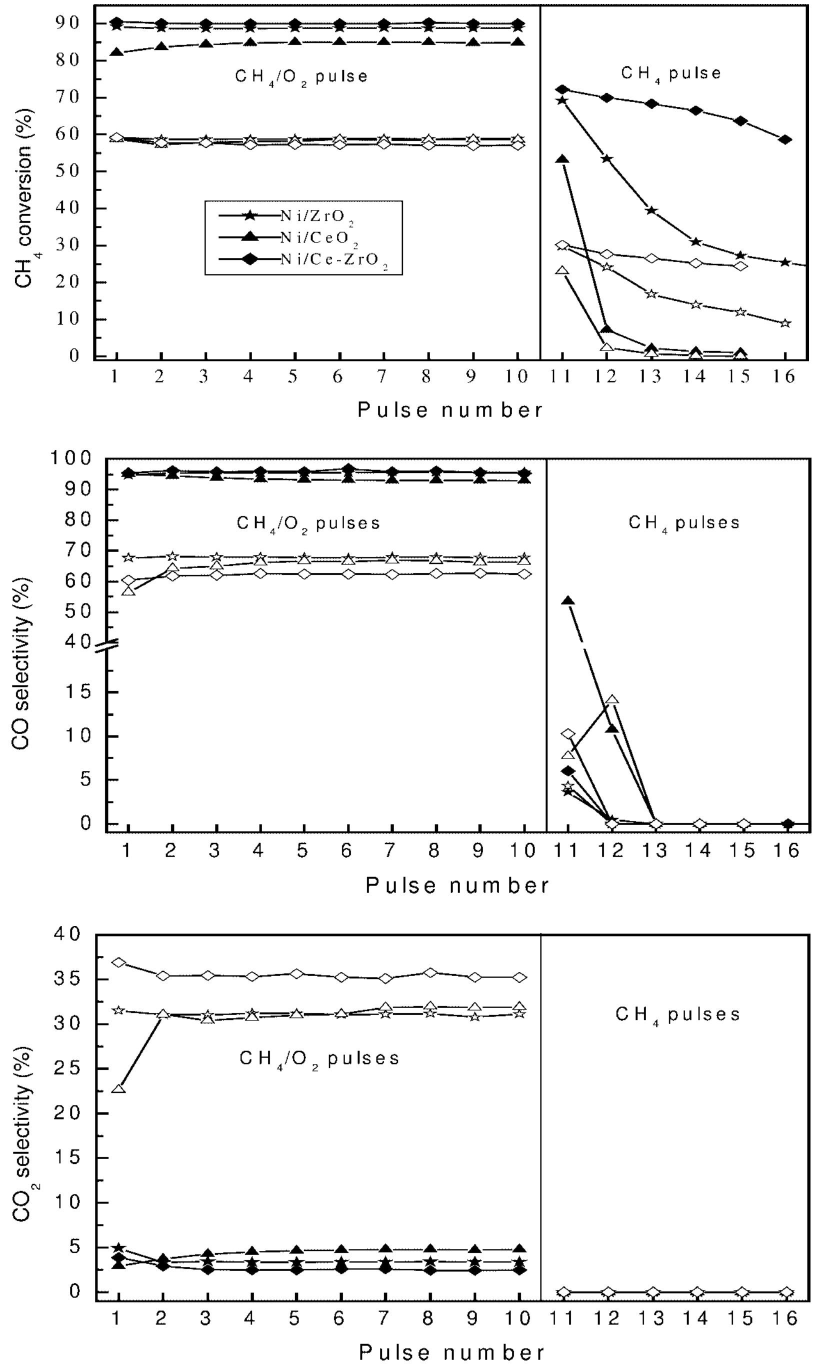

Figure 2. Pulse reaction of CH_4/O_2 (2/1) or CH_4 over Ni/CeO_2, Ni/ZrO_2 and $Ni/Ce–ZrO_2$ catalysts. Solid symbols 800 °C, hollow symbols 600 °C.

After ten pulses of CH_4/O_2, pure CH_4 was injected. In the first CH_4 pulse, a considerable amount of CO was formed, but no CO_2 was detected over all the catalysts. The results indicate that some oxygen species were still present on the catalysts after CH_4/O_2 pulses, and these oxygen species are favorable to CO formation. Thus, it is reasonable that the adsorbed oxygen species also constitute the intermediate in the CH_4/O_2 partial oxidation. Among the catalysts, Ni/CeO_2 showed the highest CO selectivity and yield, indicating that Ni/CeO_2 has the largest capacity of oxygen storage. This is possibly why Ni/CeO_2 catalyst showed the lowest CO selectivity during the set of CH_4/O_2 pulse reaction.

When CH_4/O_2 pulse reaction was carried out at 600 °C, all the catalysts showed similar CH_4 conversions. The activity of CH_4 dissociation over these supported Ni catalysts was not directly related with the reaction activity in CH_4/O_2 pulse. Hu and Ruckenstein [12] suggested that the reaction between the surface carbon species and O species constitutes the rate-controlling step in POM. Thus, the present results can be reasonably explained by this viewpoint. Ni/CeO_2 showed 56.5% CO selectivity and 22.7% CO_2 selectivity in the first pulse, suggesting some carbon species deposit on the catalyst surface. This is mainly due to the lack of active oxygen species because some parts of oxygen were used to replenish lattice oxygen in CeO_2, which has lower activity to react with surface carbon species at 600 °C as confirmed in the subsequent pure CH_4 pulses. In the following CH_4/O_2 pulses, the CO selectivity over Ni/CeO_2 remained constant at about 67%, which is similar to that over Ni/ZrO_2. Meanwhile, $Ni/Ce–ZrO_2$ showed the lowest CO selectivity and the highest CO_2 selectivity, implying that adsorbed oxygen species at 600 °C over $Ni/Ce–ZrO_2$ are the richest. This speculation is supported by the results of the subsequent CH_4 pulses after CH_4/O_2 pulses. In the CH_4 pulse, $Ni/Ce–ZrO_2$ showed the highest CO selectivity and yield among the three catalysts as shown in figure 2.

Comparing the results of CH_4/O_2 pulses at 800 °C with those at 600 °C, CO_2 selectivities over all the catalysts decreased with increasing temperature. Shen *et al.* [14] indicated that the selectivity to CO and CO_2 in POM mainly depends on the relative concentration of surface carbon to oxygen species. Thus it can be reasonably explained as follows. Over Ni/CeO_2, Ni/ZrO_2 and $Ni/Ce–ZrO_2$ catalysts, oxygen and methane adsorb competitively on metallic nickel. Methane adsorption on Ni is an activation process and the adsorption rate can be accelerated by increasing temperature, whereas the surface coverage of adsorbed O species decreases with rising temperature, thus resulting in the decrease of CO_2 selectivity. On the other hand, CO_2 formation and CO selectivity are also governed by the two competition steps, namely the oxidation of CO(s) to CO_2 and the desorption of CO(s) to CO(g). The increase of reaction temperature would rather favor CO(s) desorption other than CO(s) oxidation, leading to the increase of CO selectivity [11].

4. Discussion

4.1. Mechanistic schemes of POM over Ni/CeO_2 and Ni/ZrO_2 catalysts

In our previous studies [18], H_2 pulse chemisorption indicated that H_2 uptake over Ni/CeO_2, Ni/ZrO_2 and $Ni/Ce–ZrO_2$ are 0.0, 12.8, 9.39 μmol/g-cat, respectively. Maubert *et al.* [20] also found that hydrogen chemisorption on Ni/CeO_2 was decreased significantly after high temperature reduction. They suggested that a SMSI-like interaction takes place in the $Ni–CeO_2$ system, resulting from geometric and/or electronic effect. The strong interaction between Ni and ceria may result in a large extent of boundary between CeO_2 and Ni. When freshly reduced Ni/CeO_2 catalyst was exposed to CH_4 pulses, the formation of a large amount of CO was observed. The formation of CO was from the reaction between adsorbed CH_x species with lattice oxygen species in the CeO_2 support since there is no gas-phase oxygen species present in the system. During CH_4 pulses, some carbon species were deposited on the catalyst surface. Once the carbon species deposit on the catalyst surface they are very difficult to remove as confirmed by the results of the subsequent pulses of O_2. During the O_2 pulses, a very small amount of CO and CO_2 was produced, while a large amount of carbon species still remained on the catalyst surface. This result supports the idea that CO is mainly produced from the reaction between adsorbed carbon species and lattice oxygen of the CeO_2 support in the vicinity of the Ni/CeO_2 interface under the present reaction condition. These results support the following mechanism (see figure 3). CH_4 adsorbs on the metallic Ni and then dissociates further to give H_2 and carbon species (CH_x, $x = 0–3$), which can easily migrate to the interface of $Ni–CeO_2$ due to the large extent of the boundary between CeO_2 and Ni, and reduce CeO_2 support near the metallic nickel particle to produce CO or, in the absence of reducible lattice oxygen, form carbon deposition on the metallic Ni or migrate to the surface of CeO_2 support. The second path is the dissociation of O_2. The lattice oxygen removed by the reaction with carbon species can be replenished by the gas-phase oxygen *via* a redox mechanism. The balance between the rate of CH_4 decomposition and the cleaning rate of carbon species by the reducible lattice oxygen in the CeO_2 support determines the overall stability of the catalyst.

Over Ni/ZrO_2 catalyst, the amount of mobile oxygen species in ZrO_2 support is very scarce as indicated by our previous studies [21]. This suggests that the contribution

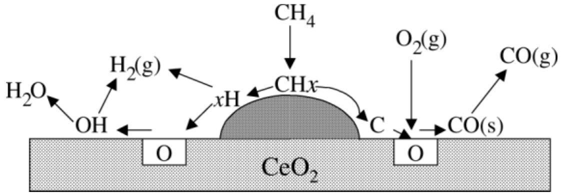

Figure 3. The mechanistic scheme for POM over Ni/CeO_2 catalyst.

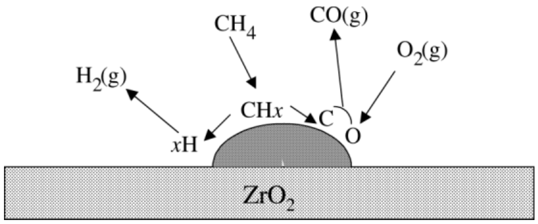

Figure 4. The mechanistic scheme for POM over Ni/ZrO$_2$ catalyst.

of lattice oxygen to CO production during the reaction is very small. The results of CH$_4$ pulses over freshly reduced Ni/ZrO$_2$ presented in figure 1 provide evidence for this speculation. Consistently, our previous TPR results [16] indicated that there is no obvious reduction peak for ZrO$_2$ up to 900 °C. However, we cannot totally exclude the possibility that the lattice oxygen participates in the reaction through partial reduction of zirconia at high temperatures. In fact, a large amount of CO together with a small amount of CO$_2$ was observed when CH$_4$ was pulsed over Pt/ZrO$_2$ catalyst [22]. It was suggested that ZrO$_2$ over the Pt/ZrO$_2$ catalyst can be partially reduced by the carbon produced from the decomposition of methane. A similar effect of zirconia is also observed in the study of CO$_2$ reforming with methane [23,24]. However, in the present work, a very small amount of CO was produced and there was no detectable CO$_2$ although the CH$_4$ conversion was very high (figure 1). Moreover, there was no carbon-containing gaseous products detected after the second CH$_4$ pulse. Thus we can conclude that CO is mainly produced over Ni/ZrO$_2$ by the reaction between carbon and oxygen species adsorbed on the metallic nickel surface, although the contribution of the lattice oxygen of zirconia support, which is similar to the mechanism shown in figure 3, cannot be excluded totally. The most likely mechanistic scheme is illustrated in figure 4.

4.2. Cerium promotion

The results presented in this paper clearly show that the addition of ceria enhances the CH$_4$ dissociation, improves the carbon capacity and promotes carbon elimination of the catalyst. The promotional effects of ceria may stem from the following reasons.

Figure 1 shows that the addition of ceria enhances the CH$_4$ dissociation ability of the catalyst, implying that the amount of metallic nickel exposed for the reaction increases, although the previous results of H$_2$ pulse chemisorption [18] indicated that H$_2$ uptake over Ni/Ce–ZrO$_2$ is less than that over Ni/ZrO$_2$. This phenomenon can be explained by the geometric effect, *e.g.*, the migration and coverage of Ni by the partially reduced Ce oxide during the reduction procedure, which leads to the increase of H$_2$ uptake activation energy at low temperatures. Since the Ni ensembles may be separated or covered by Ce oxide during reduction, a large extent of boundary between the support and Ni would be formed. It makes the migration of carbon species to the interface of metal–support much easier, thus resulting in higher carbon storage capacity and stronger ability to resist deactivation caused by carbon deposition.

In our previous studies [18], we have characterized the calcined Ni/ZrO$_2$ and Ni/Ce–ZrO$_2$ catalysts by XRD. ZrO$_2$ in Ni/ZrO$_2$ was identified as the monoclinic phase, while the tetragonal phase is obtained for the Ni/Ce–ZrO$_2$, which indicates that the presence of CeO$_2$ in ZrO$_2$ retards or prevents the transformation from tetragonal to monoclinic as reported by other researchers [25,26]. At the same time, the XRD patterns were consistent with the presence of Ce–ZrO$_2$ solid solution, in which Zr is incorporated into the CeO$_2$ lattice and the segregation of ceria from the solid solution could not be detected by XRD. In this respect, ZrO$_2$ is stabilized through the formation of the solid solution with CeO$_2$. In parallel with the changes observed in the crystalline phases, the BET surface area of the ZrO$_2$ support (18.4 m^2/g) increased significantly to 55.0 m^2/g with the addition of ceria. It is well established that CeO$_2$ has high oxygen storage capacity (OSC), which promotes the formation of oxygen vacancies and increases the mobility of oxygen in the Ce–ZrO$_2$ solid solution [27]. This is supported by the results presented in table 1. After five oxygen pulses, the oxygen species remaining on Ni/Ce–ZrO$_2$ were much more than those on Ni/ZrO$_2$, indicating that Ni/Ce–ZrO$_2$ has higher OSC. In addition, our previous studies [16] showed that zirconia support does not show any reduction peak in TPR. While the reduction of ceria could be done at 800 °C, it could be achieved at 640 °C when ceria is present. When Ni is supported on the Ce–ZrO$_2$ support, the reduction peak of the support shifts further to lower temperature due to the H$_2$ spillover effect, indicating that the Ce oxide is much easier to reduce over Ni/Ce–ZrO$_2$. The easier reducibility of ceria makes it possible to transfer oxygen species much more effectively *via* a redox cycle [21].

The promotional effect of cerium on the oxygen transfer is also supported by the fact that the amounts of CO and CO$_2$ produced over Ni/Ce–ZrO$_2$ in the third set of the CH$_4$ pulse as shown in figure 1 were higher than those over Ni/ZrO$_2$ catalyst.

The strong ability to store, release and transfer oxygen species results in an enhanced ability to clean carbon that would normally accumulate on the Ni surface during the decomposition of CH$_4$, as confirmed by the results presented in table 1. After five CH$_4$ pulses, the amount of carbon deposited on Ni/Ce–ZrO$_2$ was the highest; the residue carbon after five O$_2$ pulses was the lowest. This result clearly shows that the ability to eliminate carbon species on Ni/Ce–ZrO$_2$ is the best. Similar results have been observed on Pt/Ce–ZrO$_2$ for the CO$_2$ reforming methane and Ni/Ce–Al$_2$O$_3$ catalyst for the steam reforming reaction [19,28].

Based on the above results and discussion, the reaction scheme over Ni/Ce–ZrO$_2$ can be reasonably proposed as follows (see figure 5). CH$_4$ adsorbs on the Ni surface and then dissociates further to give H$_2$ and carbon species. Some carbon species react with oxygen species which are activated on the metallic Ni to produce CO, while some may migrate

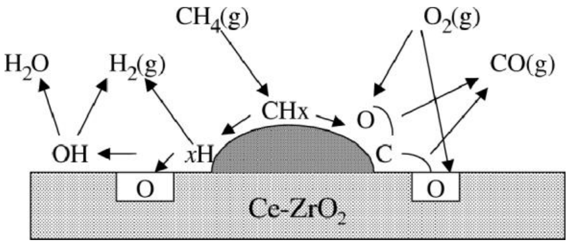

Figure 5. The mechanistic scheme for POM over Ni/Ce–ZrO_2 catalyst.

to the interface of Ni–Ce–ZrO_2 due to the large extent of the boundary between Ce–ZrO_2 and Ni, and reduce the support near the metallic nickel particle to produce CO. Both these two routes contribute to the production of CO. The adsorbed oxygen species on the metallic Ni and the lattice oxygen in the Ce–ZrO_2 support, which are removed from the reaction with carbon species, can be replenished by the gaseous oxygen.

5. Conclusions

The following are the conclusions drawn out of this investigation.

(1) Over Ni/CeO_2 catalyst, CH_4 dissociates on the metallic nickel, and CH_x species migrate rapidly to the interface of Ni–CeO_2, then reduce the CeO_2 support near the metallic nickel particle to produce CO. This is a main route for CO formation. Lattice oxygen can be replenished with gas-phase oxygen by a redox cycle.

(2) Over Ni/ZrO_2, both CH_4 and O_2 are activated on the surface of the metallic Ni, and then adsorbed carbon reacts with adsorbed oxygen to produce CO. This is the main path for POM at present conditions.

(3) The addition of ceria to zirconia enhances the activity of the catalyst for CH_4 dissociation and improves the carbon storage capacity. Moreover, it increases the storage capacity and mobility of oxygen in the catalyst, thus promoting carbon elimination.

References

[1] M.A. Peña, J.P. Gómez and J.L.G. Fierro, Appl. Catal. A 144 (1996) 7.
[2] A.T. Ashcroft, A.K. Cheetham, M.L.H. Green and P.D.F. Vernon, Nature 352 (1991) 225.
[3] D.A. Hickman and L.D. Schmidt, Science 259 (1993) 343.
[4] V.R. Choudhary, A.M. Rajput and B. Probhaker, J. Catal. 139 (1993) 326.
[5] S.C. Tsang, J.B. Claridge and M.L.H. Green, Catal. Today 23 (1995) 3.
[6] A.M. Diskin, R.H. Cunningham and R.M. Ormerod, Catal. Today 46 (1998) 147.
[7] S. Tang, J. Lin and K.L. Tan, Catal. Lett. 51 (1998) 169.
[8] D. Dissanayake, M.P. Rosynek, K.C.C. Kharas and J.H. Lunsford, J. Catal. 132 (1991) 117.
[9] W.J.M. Vermeiren, E. Blomsma and P.A. Jacobs, Catal. Today 13 (1992) 427.
[10] K. Heitnes, S. Lindberg, O.A. Rokstad and A. Holmen, Catal. Today 24 (1995) 211.
[11] C.T. Au, H.Y. Wang and H.L. Wan, J. Catal. 158 (1996) 343.
[12] Y.H. Hu and E. Ruckenstein, J. Catal. 158 (1996) 260.
[13] Y. Lu, J. Xue, C. Yu, Y. Liu and S. Shen, Appl. Catal. A 174 (1998) 121.
[14] S. Shen, C. Li and C. Yu, Stud. Surf. Sci. Catal. 119 (1998) 765.
[15] R. Jin, Y. Chen, W. Li, Y. Ji, C. Yu and Y. Jiang, Appl. Catal. A 201 (2000) 71.
[16] H.-S. Roh, W.-S. Dong, K.-W. Jun and S.-E. Park, Chem. Lett. (2001) 88.
[17] J.-S. Chang, S.-E. Park and H. Chon, Appl. Catal. A 145 (1996) 111.
[18] H.-S. Roh, K.-W. Jun, W.-S. Dong, S.-E. Park and Y.-S. Baek, J. Mol. Catal., in press.
[19] S.M. Stagg-Williams, F.B. Noronha, G. Fendley and D.E. Resasco, J. Catal. 194 (2000) 240.
[20] A. Maubert, G.A. Martin, H. Praliaud and P. Turlier, React. Kinet. Catal. Lett. 24 (1984) 183.
[21] H.-S. Roh, K.-W. Jun, W.-S. Dong, S.-E. Park and Y.-S. Baek, Catal. Lett. 74 (2001) 31.
[22] S.M. Stagg, E. Romeo, C. Padro and D.E. Resasco, J. Catal. 178 (1998) 137.
[23] A.M. Efstathiou, A. Kladi, V.A. Tsipouriari and X.E. Verykios, J. Catal. 158 (1996) 64.
[24] E.S. Putna, T. Bunluesin, X.L. Fan, R.J. Gorte, J.M. Vohs, R.E. Lakis and T. Egami, Catal. Today 50 (1999) 343.
[25] F.B. Noronha, E.C. Fendley, R.R. Soares, W.E. Alvarez and D.E. Resasco, Chem. Eng. J. 82 (2001) 21.
[26] J.A. Montoya, E. Romero-Pascual, C. Gimon, P.D. Angel and A. Monzon, Catal. Today 63 (2000) 71.
[27] M.H. Yao, R.J. Baird, F.W. Kunz and T.E. Hoost, J. Catal. 166 (1997) 67.
[28] Q. Zhuang, Y. Qin and L. Chang, Appl. Catal. 70 (1990) 1.